2017 IEEE International Conference on Advanced Intelligent Mechatronics (AIM)
Sheraton Arabella Park Hotel, Munich, Germany, July 3-7, 2017

Analysis and robust control design of a steering system for autonomous vehicles

Balázs Németh, Dániel Fényes, Péter Gáspár, András Mihály

***Abstract*— The paper proposes the analysis and control of a steering system which is linked to the requirements of autonomous vehicles. The steering system of an autonomous vehicle must guarantee reliable and highly efficient intervention even in extreme conditions. Therefore, the determination of the reachability domain of the steering system is important. Both simulations and frequency domain methods are applied to the calculation. The paper shows that the reachability domain significantly depends on both the steering angle and the steering speed, which is utilized in the steering control design. Two results are incorporated in the robust control design of the steering. First, the analysis results of the steering system are built into the robust $\mathcal{H}_\infty$ control design through frequency-dependent weighting functions. Second, experimental vehicle tests have been performed to examine the steering style of the driver. This information is also incorporated in the steering control through preview information. Finally, high-fidelity simulation scenarios show that the proposed method has several advantages compared to the conventional steering control solution.**

I. Introduction and motivation

In the last decade the autonomous vehicle systems have had significant impact on the research of vehicle control. Several intelligent sensors and actuators are built in the vehicles in order to monitor the traffic environment, e.g., virtual sensors applying the cloud technology with internet connection. These signals are applied in the design of the control systems and vehicle functions.

Steering is one of the most important components in the autonomous vehicle since it is able to guarantee lateral stability and trajectory tracking. Several papers deal with the design of intelligent steering systems, which must be precise and fast for safe cruising. The modeling and analysis of the electric power steering system are proposed by [1]. In that research the effects of the steering on vertical dynamics are in the focus. A fault-tolerant tracking control for four-wheel steering autonomous vehicles is presented by [2]. Generally, the control system requires signals about the road in order to monitor the road conditions. However, [3] proposes a control design based on a multiple model adaptive method, which does not require road information. A parameter adaptive steering control is proposed by [4]. A nonlinear model predictive control is proposed by [5], [6]. Similarly, [7] presents a method based on a model predictive envelope of the steering control, in which the physical limits are considered.

One of the main motivations of the paper is that the steering limits must be taken into consideration in the design of the autonomous steering control. [9] proposes that both the steering angle and the steering speed influence the efficiency of the steering properties significantly. Figure 1 illustrates an example, in which the controllability domains of the steering actuation are computed for normal steering $\nu = 1$ and very fast steering $\nu = 30$, where ν is related to the relationship between steering angle and steering speed. In the axles α_1, α_2 are the lateral slip angles on the front and the rear wheels. The example illustrates that the actuation speed influences the domain in which the stability of the vehicle can be guaranteed using the steering input. In the case of a typical driver extremely fast steering has less probability due to the limits of the human muscle torque generation. However, in the case of an autonomous control system the steering speed must be controlled in order to improve the controllability domain of the vehicle.

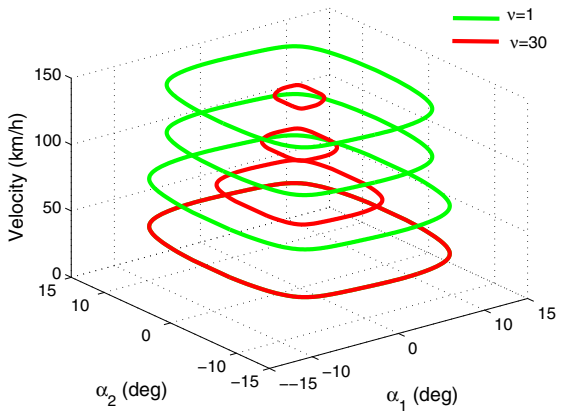

Fig. 1. Illustration of the controllability domains

This paper proposes a novel design method for the robust steering control. The analysis of the steering dynamics is based on the calculation of the controllability domains. The analysis results of the steering system are considered in the robust $\mathcal{H}_\infty$ control design through the frequency

B. Németh, D. Fényes are with Systems and Control Laboratory, Institute for Computer Science and Control, Hungarian Academy of Sciences, Kende u. 13-17, H-1111 Budapest, Hungary. E-mail: [balazs.nemeth]@sztaki.mta.hu

P. Gáspár and A. Mihály are with Institute for Computer Science and Control, Hungarian Academy of Sciences and MTA-BME Control Engineering Research Group, Budapest, Hungary. E-mail: peter.gaspar@sztaki.mta.hu

The research was supported by the National Research, Development and Innovation Fund through the project "SEPPAC: Safety and Economic Platform for Partially Automated Commercial vehicles" (VKSZ 14-1-2015-0125).

This paper was partially supported by the János Bolyai Research Scholarship of the Hungarian Academy of Sciences.

dependent weighting functions. Furthermore, in the steering control the preview of the forthcoming road sections based on experimental tests, which represent the driver's style in the steering, is considered. The novelty of the paper is the robust control method, in which these two design factors are involved.

The paper is organized as follows. Section II proposes the analysis of the steering system, in which the actuation speed is examined. The design of the steering system using the robust $\mathcal{H}_\infty$ control method is proposed in Section III. The efficiency of the design method is illustrated through simulation examples, see Section IV. Finally, Section V summarizes the conclusions of the paper.

II. Analysis of the steering dynamics

The steering has significant impact on the dynamics of the vehicle through the steering angle and the steering speed, as illustrated in the previous section. In the following the relationship between the steering angle, the steering speed and the impact of the steering manoeuvre on the vehicle dynamics is examined.

The lateral dynamics of the vehicle is described by the bicycle model, which incorporates a steady-state representation of the tire dynamics, see [10]. However, the analysis of the steering speed shows that tire dynamics has significant impact on vehicle dynamics. The dynamics of the tire is analysed in [11]. The nonlinearities of the tire characteristics are described as follows:

$$\dot{F}_{i,y} = -\frac{v}{L_i} F_{i,y} + \frac{C_{i,1}(\alpha_i) v}{L_i} \alpha_i + C_{i,0}(\alpha_i) \qquad (1)$$

where $i \in \{f, r\}$ is the index of front and rear axles, respectively. $L_i = C_{i,1}/s_i$ is the relaxation length, which is generally in the range $0.3 \ldots 0.7$. Furthermore, s_i is the tire stiffness, $C_{i,1}(\alpha_i)$ is the cornering stiffness and $C_{i,0}(\alpha_i)$ is constant, v is the vehicle velocity and α_i is the lateral slip of the front axle. In the model the nonlinearities of the tire characteristics are considered as dependency on the tire side slip through $C_{i,0}(\alpha_i), C_{i,1}(\alpha_i)$. These values are modified continuously through the analysis, depending on the current α_i, see [12].

The dynamics of the vehicle is formulated as

$$mv(\dot{\psi} + \dot{\beta}) = F_{f,y} + F_{r,y} \qquad (2a)$$

$$J\ddot{\psi} = F_{f,y} l_f - F_{r,y} l_r \qquad (2b)$$

where J is the yaw inertia of the vehicle, m is the vehicle mass and l_f, l_r are geometric parameters, the signal β is the side-slip, $\dot{\psi}$ is the yaw-rate and the steering angle is represented by δ. Moreover, there is a relationship between α_i and $\dot{\psi}, \beta$, such as $\alpha_f = \delta - \beta - \frac{\dot{\psi} l_f}{v}$ and $\alpha_r = -\beta + \frac{\dot{\psi} l_r}{v}$.

Based on the nonlinear model of the vehicle and the tire several simulations are performed to obtain the approximation of the reachability domain of the steering system at different velocities. In the simulations sinus steering signals with constant amplitude δ_{max} have been applied. The simulations have been performed with different constant steering speeds $\dot{\delta}$. The purpose of the simulations is to examine the yaw-rate $\dot{\psi}$ and side-slip β trajectories of the vehicle, which results in the simulation-based approximation of the reachability domain on the function of the actuation speed.

Figure 2 illustrates an example of the reachability domain at $v = 70km/h$ and $\delta_{max} = 6°$. Based on the simulations the convex hulls of the $\dot{\psi} - \beta$ trajectories have been fitted and the results are illustrated. It can be seen that the reachability domains significantly differ as functions of the different steering speeds $\dot{\delta}$. The reachability domain slightly increases between $1 \ldots 10\ rad/s$, while the domain decreases at higher steering speed, see Figure 2.

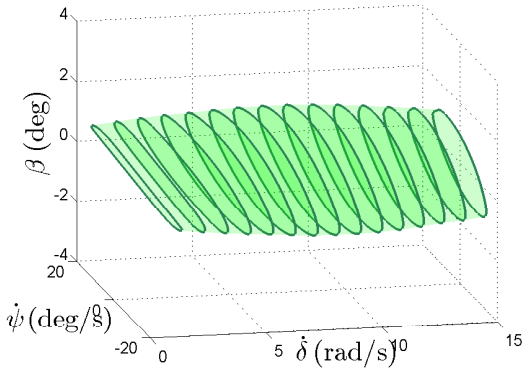

Fig. 2. Illustration of the reachable domain $v = 70km/h$

The deformation in the reachability region is more significant at higher velocities, e.g., at $v = 100km/h$, see Figure 3. In this case the reachability domain increases significantly between $1 \ldots 8rad/s$, and its shape significantly changes. Moreover, if $\dot{\delta} > 8rad/s$ then the domain decreases, see Figure 3.

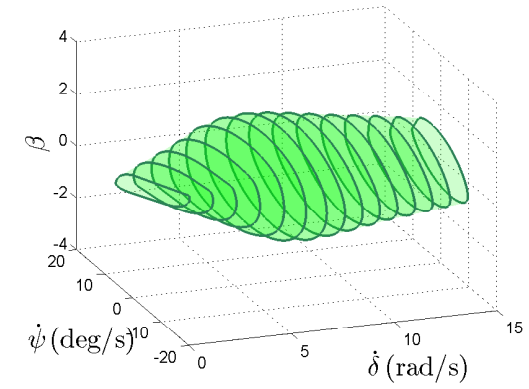

Fig. 3. Illustration of the reachable domain $v = 100km/h$

In the next simulation the velocity of the vehicle is $v = 130km/h$, which represents a fast cruising scenario. Figure 4 shows that the tendency of the reachability domains is similar to in the previous scenarios. However, at high velocity the modification of the size of the reachability domains is more significant, see the results of the simulations $\dot{\delta} = 1rad/s$ and $\dot{\delta} = 7rad/s$.

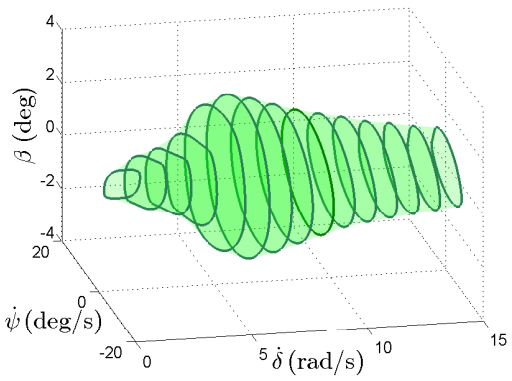

Fig. 4. Illustration of the reachable domain $v = 130km/h$

The examples show that the reachability domain as functions of the steering speed can be calculated. Based on the simulation results, in summary it can be stated that the reachability domain can significantly depend on the steering speed. Consequently, the efficiency of the steering actuations as functions of the vehicle dynamics can be considered in the design. Note that there is a relationship between the reachability domain and the controllability domain, see e.g., [13].

In the following the variation of the reachability sets is examined through a frequency-based method. In the previous example the frequency of the sinus steering actuation is modified, which results in the change of the reachability domains. In the following the system (1) and (2) will be analyzed in the frequency domain. The purpose of the analysis is to find the gains of the steering system in the frequency domain. Thus a linear model is formed by using $C_{i,0}(\alpha) = 0$ and $C_{i,1}(\alpha) = C_i$ the maximum singular value is computed in the frequency domain. This function provides information about the gains of the steering system, i.e., $\dot{\delta}$. Although the frequency domain analysis is based on the linearized model of the system, it has analogy to the reachability domain.

Figure 5 illustrates the maximum singular values of the lateral dynamics at different velocities. There are significant modifications in the trend of the maximum singular values around the frequency breakpoint. If the velocity increases, the modification is more significant. It has the same impact as the velocity on the reachability domain. Moreover, the modification of the singular values is close to the steering speed, where the reachability domains vary significantly. Thus, the frequency domain analysis provides an approximation of the variation of the reachability domain. Consequently, the frequency domain analysis provides a preliminary evaluation of the steering system. Moreover, the frequency domain information can be more easily incorporated in the control design, as it will be shown in the paper.

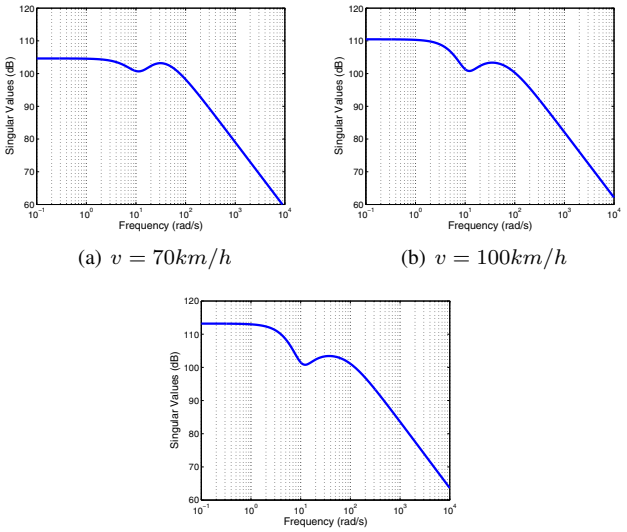

(a) $v = 70km/h$ (b) $v = 100km/h$

(c) $v = 130km/h$

Fig. 5. Singular values of the system

III. Robust control design of autonomous steering

The purpose of the steering control design is to guarantee the cruising of the vehicle, in which the steering intervention is similar to the driver's actuation. It must guarantee the comfort of the passengers and provides predictability for the drivers of the conventional vehicles and the pedestrians. To provide knowledge about the human steering style a driving test through real road tests has been performed. A project for adding autonomous vehicle features, together with associated automatic control, to a production electric car, was launched by the Institute for Computer Science and Control in 2016.

The purpose of the test scenario was the analysis of the driver steering behavior, while several signals were measured, e.g., the GPS position, the velocity, the acceleration and the steering angle and, simultaneously, the environment of the vehicle was monitored through a camera and LiDAR. Figure 6 shows a short road section of a real test scenario, which was performed around Budapest. Contributions of the test are that the preview has an important role in the human steering intervention and it must be built in the autonomous lateral control.

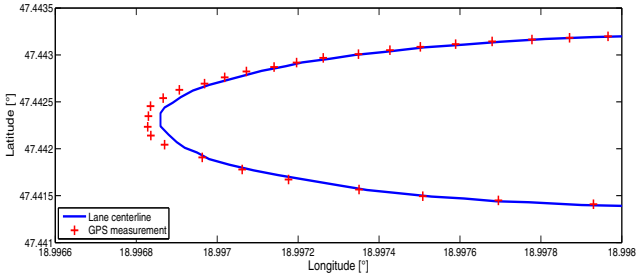

Fig. 6. Track of the vehicle in a bend

The steering angle δ of the autonomous control is divided into two parts, such as

$$\delta = \delta_a + \delta_p \tag{3}$$

where δ_a is the steering angle, which represents the input, generated from the current information $e_{y,a}$ and $e_{\psi,a}$. The steering angle δ_p is computed from the predicted errors $e_{p,i}$, resulting from the preview information. In the following the design of δ_a and the computation of δ_p are presented.

A. Design of the current steering component δ_a

The design of δ_a is based on the vehicle model, which incorporates the lateral dynamics, whose nonlinear form is in Section II, see (2). For the control design it is linearized around small slip values and the dynamics of the tire is ignored. As a result $C_{i,0}(\alpha) = 0$ and $C_{i,1}(\alpha) = C_i$ are considered. Thus, the resulting linear form is

$$m\ddot{y} = C_f\left(\delta_a - \frac{\dot{\psi}l_f + \dot{y}}{v}\right) + C_r\left(\frac{\dot{\psi}l_r - \dot{y}}{v}\right) \tag{4a}$$

$$J\ddot{\psi} = C_f l_f\left(\delta_a - \frac{\dot{\psi}l_f + \dot{y}}{v}\right) - C_r l_r\left(\frac{\dot{\psi}l_r - \dot{y}}{v}\right). \tag{4b}$$

The signal $\dot{y}$ is the lateral speed, which can be written as $\dot{y} = v\beta$. The equations (4) can be transformed into a state-space representation, where the state vector is $x = \begin{bmatrix}\dot{\psi} & \dot{y} & \psi & y\end{bmatrix}^T$, the control input is $u = \delta_a$. The state equation is written as

$$\dot{x} = Ax + Bu, \tag{5}$$

where the matrices contain the parameters of (4):

$$A = \begin{bmatrix} \frac{-C_f l_f^2 - C_r l_r^2}{Jv} & \frac{-C_f l_f + C_r l_r}{Jv} & 0 & 0 \\ \frac{-C_f l_f + C_r l_r}{mv} - v & \frac{-C_f - C_r}{mv} & 0 & 0 \\ 1 & 0 & 0 & 0 \\ 0 & 1 & 0 & 0 \end{bmatrix}, B = \begin{bmatrix} \frac{C_f l_f}{J} \\ \frac{C_f}{m} \\ 0 \\ 0 \end{bmatrix}.$$

The role of the steering angle δ_a is to guarantee the tracking of the vehicle. It results in the performance

$$z_1 = e_{y,a}, \qquad |z_1| \to min. \tag{6}$$

The appropriate trajectory tracking also requires the minimization of the heading error

$$z_2 = e_{\psi,a}, \qquad |z_2| \to min. \tag{7}$$

Moreover, the results of the analysis is considered through the control input. Therefore, a third performance is defined as

$$z_3 = \delta_a, \qquad |z_3| \to min. \tag{8}$$

The defined three performances are formed in a vector $z = \begin{bmatrix}z_1 & z_2 & z_3\end{bmatrix}^T$. Thus, the state-space representation (5) can be extended with z and the measured signals $y_m = \begin{bmatrix}\dot{\psi} & y\end{bmatrix}^T$:

$$\dot{x} = Ax + Bu \tag{9a}$$

$$z = C_1 x \tag{9b}$$

$$y_m = C_2 x + Du \tag{9c}$$

where $C_{1,2}, D$ are matrices of the performances and the measurements.

The performances of the system (9) are guaranteed by the robust $\mathcal{H}_\infty$ method. The control design is based on a weighting strategy, which is formulated through a closed-loop interconnection structure, see Figure 7. The interconnection structure contains several weighting functions, whose roles are to guarantee the trade-off between the performances and to scale the signals. The weights $W_{w,1}, W_{w,2}$ are related to the sensor characteristics of the lateral error and yaw error measurement. The role of $W_{r,1}, W_{r,2}$ is to scale the reference signals. These weights are formed as constant values. $W_{z,1}$ and $W_{z,2}$ are the weights for the performances, which represent the minimization of z_1 and z_2, see (6), (7). These are chosen in the frequency-domain form $W_{w,i} = A_i \frac{\epsilon_{2,i}s^2 + \epsilon_{1,i}s + 1}{T_{2,i}s^2 + T_{1,i}s + 1}$, where $A_i, \epsilon_{1,i}, \epsilon_{2,i}, T_{1,i}$ and $T_{2,i}$ are design parameters.

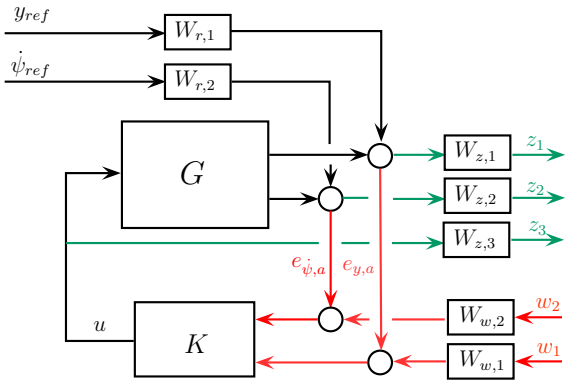

Fig. 7. Closed-loop interconnection

The performance z_3 has an important role in the design of the steering control. The analysis of the steering system resulted an analogy between the reachability domain and the frequency domain. The role of $W_{z,3}$ is to incorporate in the information of the maximum singular value function in the control design. It can result in the enhancement of the reachability of the steering actuation. Thus, if there is a significant modification in the maximum singular value function (as illustrated e.g. in Figure 5), then the weighting of the control input in that frequency region must be reduced. As a consequence of this weighting strategy in the requested frequency range the actuation δ is increased. The weight $W_{z,3}$ is formulated as

$$W_{z,3} = \delta_{d,max}\frac{\left(\frac{1}{T_2}s+1\right)^2\left(\frac{1}{T_3}s+1\right)^2}{\left(\frac{1}{T_1}s+1\right)^2\left(\frac{1}{T_4}s+1\right)^2}, \tag{10}$$

where $\delta_{d,max}$ is the maximum permitted steering wheel angle. Moreover, T_1, T_2 T_3 and T_3 are design parameters, which have role in the limitation of the steering wheel angle frequency. In Figure 8 the Bode magnitude plot of $W_{z,3}$ is illustrated. The δ_a actuation has a preferred range, which is between $T_1 \dots T_4$. Since the reachability domains are reduced at smaller and higher frequency actuation, $W_{z,3}$ has a high value out of the frequency range $T_1 \dots T_4$.

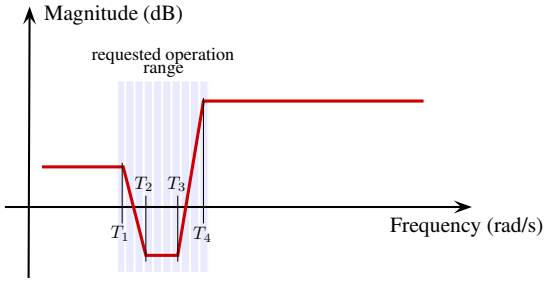

Fig. 8. Weighting of δ_a

The control design is based on the $\mathcal{H}_\infty$ methods. The objective of the control is to minimize the $\mathcal{H}_\infty$-norm of the cosensitivity function $T_{z_{lat}w}$. It is necessary to find an admissible control K_{lat} which satisfies the following design criteria: the closed-loop system must be asymptotically stable and the closed-loop transfer function from the disturbance w_l to the performance z_{lat} satisfies the following constraint

$$\left\| T_{z_{lat}w_l} \right\|_\infty < \gamma, \tag{11}$$

for a given real positive value γ. The result of the optimization problem is used to calculate the steering angle δ_a. The solution of the optimization is standard, see [15], [16].

B. Design of the predicted steering component δ_p

The design of δ_p results from the error of the predicted road section. In the prediction two look-ahead points are considered, which are important for the driver. Based on the results of scenarios with real vehicle tests, the first point from the current position of the driver is $T_{p,1} = 0.53\ sec$ ahead, while the second point is $T_{p,2} = 0.93\ sec$, see [17].

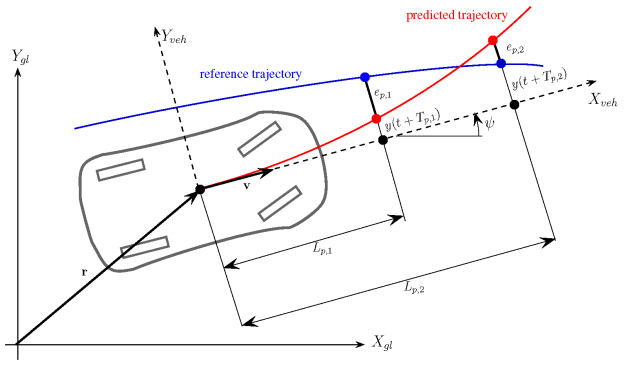

Fig. 9. Prediction of the oncoming trajectory

The prediction of the lateral error in $T_{p,i}$ requires the prediction of the motion, see Figure 9. The position of the vehicle in the coordinate system of the vehicle at the time $t+T_{p,i}$ is computed using the Taylor series technique. It can result in a good approximation of the trajectory for $n = 2$, such as

$$y(t+T_{p,i}) = \sum_{n=0}^{\infty} \frac{y^n(t)}{n!} T_{p,i}^n \approx$$
$$\approx y(t) + \dot{y}(t) T_{p,i} + \frac{1}{2}\ddot{y}(t) T_{p,i}^2 \tag{12}$$

Considering that the longitudinal velocity is constant, the prediction horizon for $T_{p,i}$ is computed as $L_{p,i} = vT_{p,i}$. Thus, the position vector of the vehicle at the time $t + T_{p,i}$ is

$$\mathbf{r_{veh}}(t+T_{p,i}) = \begin{bmatrix} L_{p,i} \\ y(t+T_{p,i}) \end{bmatrix} \tag{13}$$

The computation of the predicted position of the vehicle in the global coordinate system $\mathbf{r_{gl}}$ requires the rotation of the vector $\mathbf{r_{veh}}(t+T_{p,i})$ with the current yaw angle $\psi(t)$ and its addition to the current position $\mathbf{r}(t)$. Thus, the resulting position is

$$\mathbf{r_{gl}}(t+T_{p,i}) = \mathbf{r}(t) + \begin{bmatrix} L_{p,i}\cos\psi(t) - y(t+T_{p,i})\sin\psi(t) \\ L_{p,i}\sin\psi(t) + y(t+T_{p,i})\cos\psi(t) \end{bmatrix} \tag{14}$$

The errors $e_{p,1}$, $e_{p,2}$ result in the difference between the reference position $\mathbf{r_{ref}}(t+T_{p,i}) = \begin{bmatrix} x_{ref}(t+T_{p,i}) & y_{ref}(t+T_{p,i}) \end{bmatrix}^T$ and the predicted positions $\mathbf{r_{gl}}(t+T_{p,i})$. The reference positions are defined as the intersection of the reference trajectory and the perpendicular on the vehicle direction x, see Figure 9. The errors are computed using (14) as the length of the resulting vector difference as

$$\mathbf{e_i} = \mathbf{r_{ref}}(t+T_{p,i}) - \mathbf{r_{gl}}(t+T_{p,i}) \tag{15a}$$
$$e_{p,i} = \left| \mathbf{e_i} \right| \tag{15b}$$

The predicted steering angle δ_p component is computed as the weighted sum of the errors using (15b), such as

$$\delta_p = K_{p,1} e_{p,1} \cdot sign(z_{p,1}) + K_{p,2} e_{p,2} \cdot sign(z_{p,2}) \tag{16}$$

where $K_{p,1}$ and $K_{p,2}$ are the weights and $sign(z_{p,i})$ represents the direction of the lateral error $e_{p,i}$. The value $z_{p,i}$ is the coefficient of the vertical component, resulting in the cross product $\mathbf{v} \times \mathbf{e_i}$, where $\mathbf{v}$ is the vector of the longitudinal velocity.

IV. Demonstration of the Steering Control

Finally, the efficiency of the proposed method in the design of the steering system is shown in this section. The goal of the simulation scenarios is to demonstrate that the proposed control design is able to influence the dynamics of the steering signal through the weighting in the frequency range. The simulations are performed in the high-fidelity vehicle dynamic software CarSim, in which a mid-size D-class passenger vehicle is selected.

In the example two control strategies are compared to each other. First, in the control design the frequency dependency in the weighting functions is not considered, which results in the constant $W_{z,3} = 0.3$. This scenario results in the control K_1. However, in the second design the frequency-dependent weighting functions are applied, which results in the control K_2. Here the weighting function $W_{z,3}$ depends on the frequency domain such as

$$W_{z,3} = \frac{0.0001s^4 + 0.004s^3 + 0.06s^2 + 0.4s + 1}{0.0000562s^4 + 0.00487s^3 + 0.1206s^2 + 0.65s + 1} \tag{17}$$

It shows that in the steering control input signal the frequency range $6 \dots 10 rad/s$ is preferred, as Figure 10 shows.

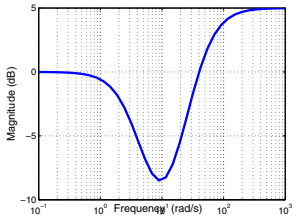

Fig. 10. Bode magnitude diagram of $W_{z,3}$

The goal of the control design is to track a reference yaw-rate signal, see Figure 11(a). It can be seen that both steering control systems are able to perform the tracking with similar errors, see Figure 11(b). Thus, the required yaw rate can be achieved using both control systems.

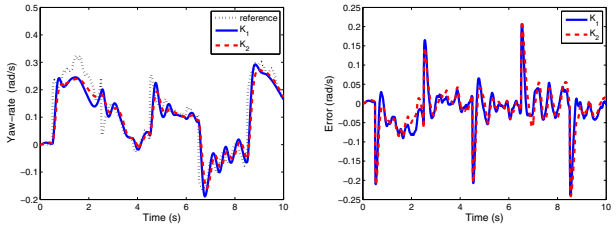

(a) Yaw-rate tracking (b) Yaw-rate error

Fig. 11. Steering interventions

The differences between the two control systems can be seen as a function of the control signal δ, see Figure 12. Figure 12(a) illustrates that K_2 requires smaller steering input compared to K_1. The similar performance, i.e., the yaw-rate tracking, can be achieved by different steering angles δ and steering speeds $\dot{\delta}$ as Figure 12(b) shown. Signal $\dot{\delta}$ illustrates the impact of W_{act} on the control design. In the case of K_1 the steering speed has high values, which is disadvantageous in terms of the reachability domain.

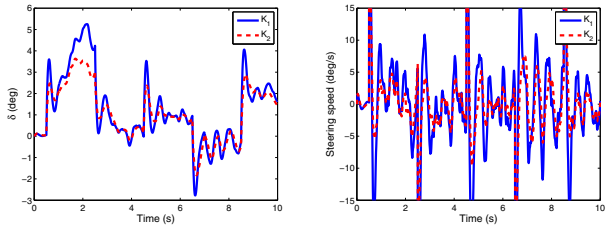

(a) Steering angle (b) Steering speed

Fig. 12. Steering interventions

V. Conclusions

The paper has proposed the analysis and control of the steering system concerning autonomous vehicles. The paper shows that the reachability domain significantly depends on the steering speed, which is utilized in the steering control design. The analysis results of the steering system are considered in the design through the frequency dependent weighting of the robust $\mathcal{H}_\infty$ control. The steering style of the driver is also incorporated in the steering control through preview information. Simulation examples show that the proposed method has several advantages compared to the conventional steering control solution. An appropriate selection of the steering speed is able to reduce the steering angle, which is advantageous in terms of the energy consumption of the autonomous steering actuator.

References

[1] Y. G. Liao and H. I. Du, "Modelling and analysis of electric power steering system and its effect on vehicle dynamic behaviour," *International Journal of Vehicle Autonomous Systems*, vol. 2, no. 1, 2003.

[2] H. Chen, Y. Song, and D. Li, "Fault-tolerant tracking control of fw-steering autonomous vehicles," *Chinese Control and Decision Conference, Mianyang, China*, pp. 92–97, 2011.

[3] T. Aoki, T. Sugimachi, T. Fukao, and H. Kawashima, "Autonomous steering control with adaptive mechanism by mmac," *Society of Instrument and Control Engineers Annual Conference, Akita, Japan*, pp. 203–210, 2012.

[4] C. Jung, H. Kim, Y. Son, K. Lee, and K. Yi, "Parameter adaptive steering control for autonomous driving," *17th International Conference on Intelligent Transportation Systems, Qingdao, China*, pp. 1462–1467, 2014.

[5] R. C. Rafaila and G. Livint, "Predictive control of autonomous steering for ground vehicles," *9th International Symposium on Advanced Topics in Electrical Engineering, Bucharest, Romania*, pp. 543–547, 2015.

[6] ——, "Nonlinear model predictive control of autonomous vehicle steering," *19th International Conference on System Theory, Control and Computing, Cheile Gradistei, Romania*, pp. 466–471, 2015.

[7] C. E. Beal and J. C. Gerdes, "Model predictive control for vehicle stabilization at the limits of handling," *IEEE Transactions on Control Systems Technology*, vol. 21, no. 4, pp. 1258–1269, 2013.

[8] M. Silva, L.Garrote, F. Moita, M. Martins, and U. Nunes, "Autonomous electric vehicle: Steering and path-following control systems," *16th IEEE Mediterranean Electrotechnical Conference, Yasmine Hammamet, Tunisia*, pp. 442–445, 2012.

[9] B. Németh, P. Gáspár, and T. Péni, "Nonlinear analysis of vehicle control actuations based on controlled invariant sets," *International Journal of Applied Mathematics and Computer Science*, vol. 26, no. 1, pp. 31–43, 2016.

[10] R. Rajamani, "Vehicle dynamics and control," *Springer*, 2005.

[11] H. B. Pacejka, *Tyre and vehicle dynamics*. Oxford: Elsevier Butterworth-Heinemann, 2004.

[12] B. Németh, P. Gáspár, and J. Bokor, "LPV-based integrated vehicle control design considering the nonlinear characteristics of the tire," *IEEE American Control Conference, Boston, USA*, 2016.

[13] D. R. Snow, *Determining reachable regions and optimal controls*, ser. Advances in Control Systems, C. T. Leondes, Ed. Academic Press, 1967, vol. 5.

[14] B. Németh, P. Gáspar, and J. Bokor, "Integrated control design based on driver-in-the-loop vehicle dynamics," in *52nd IEEE Conference on Decision and Control (CDC), Florence, Italy*, 2013, pp. 3517–3522.

[15] C. Scherer and S. Weiland, *Lecture Notes DISC Course on Linear Matrix Inequalities in Control*. Delft, Netherlands: Delft University of Technology, 2000.

[16] S. Boyd, L. E. Ghaoui, E. Feron, and V. Balakrishnan, *Linear Matrix Inequalities in System and Control Theory*. Philadelphia: Society for Industrial and Applied Mathematics, 1997.

[17] M. Land and J. Horwood, "Which parts of the road guide steering?" *Nature*, vol. 377, no. September, pp. 339–340, 1995.